Chemisorption of (CH_x and C_2H_y) Hydrocarbons on Pt(111) Clusters and Surfaces from DFT Studies

Timo Jacob and William A. Goddard III*

Materials and Process Simulation Center, Beckman Institute (139-74), California Institute of Technology, Pasadena, California 91125

Received: August 11, 2004; In Final Form: October 7, 2004

We used the B3LYP flavor of density functional theory (DFT) to study the chemisorption of all CH_x and C_2H_y intermediates on the Pt(111) surface. The surface was modeled with the 35 atom $Pt_{14.13.8}$ cluster, which was found to be reliable for describing all adsorption sites. We find that these hydrocarbons all bind covalently (σ-bonds) to the surface, in agreement with the studies by Kua and Goddard on small Pt clusters. In nearly every case the structure of the adsorbed hydrocarbon achieves a saturated configuration in which each C is almost tetrahedral with the missing H atoms replaced by covalent bonds to the surface Pt atoms. Thus, (Pt_3)-CH prefers a μ_3 hollow site (fcc), $(Pt_2)CH_2$ prefers a μ_2 bridge site, and $PtCH_3$ prefers μ_1 on-top sites. Vinyl leads to $(Pt_2)CH-CH_2(Pt)$, which prefers a μ_3 hollow site (fcc). The only exceptions to this model are ethynyl (CCH), which binds as $(Pt_2)C{=}CH(Pt)$, retaining a CC π-bond while binding at a μ_3 hollow site (fcc), and HCCH, which binds as $(Pt)HC{=}CH(Pt)$, retaining a π bond that coordinates to a third atom of a μ_3 hollow site (fcc) to form an off center structure. These structures are in good agreement with available experimental data. For all species we calculated heats of formation (ΔH_f) to be used for considering various reaction pathways on Pt(111). For conditions of low coverage, the most strongly bound CH_x species is methylidyne (CH, BE = 146.61 kcal/mol), and ethylidyne (CCH_3, BE = 134.83 kcal/mol) among the C_2H_y molecules. We find that the net bond energy is nearly proportional to the number of C−Pt bonds (48.80 kcal/mol per bond) with the average bond energy decreasing slightly with the number of C ligands.

1. Introduction

Platinum catalysts and their alloys remain the catalyst of choice for many hydrocarbon reforming and conversion processes so important in chemical and petrochemical applications.[1,2] In addition, there is increased interest in improving Pt-based catalysts for such critical applications as fuel cells. The chemistry of C_1 and C_2 hydrocarbons is important for many industrial reactions on Pt and these reactions serve as prototypes for many others. Knowledge of the structures, energetics, and barriers should be useful in characterizing the mechanisms and improving the processes. Although many experiments have characterized small hydrocarbon species on various metal surfaces,[3−6] there remains considerable uncertainty about the structures and energetics of the chemisorbed intermediates and the role they play in various reaction pathways. To aid in developing improved catalysts, it is useful to know these quantities for a complete set of reaction intermediates. This paper utilizes first principles quantum mechanics (QM) for a systematic study of the structures and energetics of these systems.

There are two general computational strategies for representing the catalyst for heterogeneous reactions: (1) a two-dimensionally infinite periodic slab with an ordered surface or (2) a finite cluster chosen to reproduce chemistry of the infinite surface or to mimic the chemistry on a dispersed catalyst.

Each approach has advantages and disadvantages. The slab is particularly useful for studying ordered overlayers and specific low index faces but describing reactions at low coverage may require a large unit cell. In addition the fastest periodic slab methods use plane-wave basis sets and do not allow the exact exchange terms needed to achieve the highest accuracy for describing chemical reactions (as in B3LYP). Also the accuracy of practical sized plane-wave basis sets for describing reactions has not been documented.

On the other hand, to represent the chemistry of realistic metal catalysts requires large clusters. Thus, in a previous study[7] (hereafter JMG), we established that the minimal cluster required to describe accurately the various sites for chemisorbing O on the Pt(111) surface must have at least 28 atoms with a minimum of three layers of atoms in each dimension. Not only does this give results similar to the infinite surface, it may well better represent highly dispersed catalysts, which might have sizes down to 2 nm diameter. Here we use Gaussian basis sets that have been well documented to describe bond dissociation processes.

In the present paper, we use the cluster approach to calculate the adsorption of all C_1H_x and C_2H_y intermediates to the (111) like facets of the cluster. To reduce edge effects for some of the larger C_2H_y species, we use the $Pt_{14.13.8}$ cluster, with 35 Pt atoms distributed over three layers.

For all C_1H_x and C_2H_y intermediates, we calculated the structures, binding energies, and vibrational frequencies of the most stable configuration. We find excellent agreement with the adsorbate geometries and character of the binding reported by Kua and Goddard (hereafter KG),[8] who modeled the surface with a single-layer Pt_8 cluster. However, the calculations with larger clusters generally lead to smaller chemisorption energies. In particular, the more extended cluster is essential for describing

* To whom correspondence should be addressed. E-mail: wag@wag.caltech.edu.

10.1021/jp0463868 CCC: $30.25
Published on Web 12/16/2004

the adsorption of the complex hydrocarbons that bind to μ_3 sites (the index indicates the coordination of the binding site), where at least three-layer clusters are necessary for accurate energetics.

To aid in considering various reaction pathways on Pt [particularly hydrogenation and decomposition of ethene on Pt(111)], we derive heats of formation (ΔH_f) for all species bound to Pt(111).

The methods are summarized in section 2. The results for 13 different C_1H_x and C_2H_y species are reported in section 3. Section 4 uses these results to establish an energetic basis for comparing various reactions and uses these results to discuss several reactions of interest. Finally, section 5 provides a summary.

2. Theoretical Methods

All calculations used the B3LYP flavor of density functional theory (DFT), in which the exchange-correlation term is a nonlocal GGA-functional (generalized gradient approximation)[9,10] that combines exact Hartree−Fock (HF) exchange with the local exchange functional of Slater.[11] In addition, it uses the Becke nonlocal gradient correction,[12] the Vosko-Wilk-Nusair exchange functional,[13] and the Lee−Yang−Parr local and nonlocal correlation functional.[10]

Among the many flavors of DFT, we prefer B3LYP because of its demonstrated accuracy for thermochemistry of organic molecules. Thus, studies by Xu and Goddard[14] comparing the thermochemistry over the G2 data set with 148 molecules with accurately experimental energies have shown that B3LYP leads to a mean average absolute error (MAD) of 0.13 eV (3.0 kcal/mol), which can be compared to other hybrid methods [PBE1PBE with 0.21 eV (4.8 kcal/mol), B3PW91 with 0.15 eV (3.5 kcal/mol)], and nonhybrid GGA methods [BLYP with 0.31 eV (7.1 kcal/mol), BPW91 with 0.34 eV (7.8 kcal/mol), PW91 with 0.77 eV (17.8 kcal/mol), and PBE with 0.74 eV (17.1 kcal/mol)]. Of course, all of these methods are much better than LDA [MAD = 3.94 eV (90.9 kcal/mol)] or HF [MAD = 6.47 eV (149.2 kcal/mol)].

Previously, we showed that BLYP (without exact exchange) leads to a bond energy for chemisorption of an O atom to the $Pt_{9.10.9}$ cluster that is only 0.06 eV (1.38 kcal/mol) weaker than for B3LYP.[7] Using the PBE functional, which is often used in combination with transition metals, the deviation in binding energy is in the same range.

All ab initio calculations were carried out with the Jaguar 4.2 program.[15] For the platinum atoms, the 60 core electrons (1s−4f) were described with the Hay and Wadt core-valence relativistic effective-core potential (ECP) leaving 18 explicit valence electrons (the atomic ground state is $(5s)^2(5p)^6(5d)^9(6s)^1(6p)^0$).[16] This uses angular momentum projection operators (nonlocal ECP) to enforce the Pauli principle.[17−20] In the Jaguar program, this ECP uses the LACVP** basis set for Pt, and all electrons for hydrogen and carbon were treated explicitly with the 6-31G** basis set.[15,16] To test whether diffuse functions on the adsorbate might be necessary, we considered previously the case of oxygen on a Pt_{28} cluster, where we found that adding diffuse functions increases the binding energy by only 0.015 eV.[7]

As discussed by KG and JMG, Pt clusters have a large number of unpaired spins resulting from the unpaired d orbitals [most Pt have a $5d^9$ configuration]. For example, we find that the ground state of the Pt_{35} cluster with 14 surface Pt atoms has a total spin of $S = 11$ (22 unpaired electrons coupled to high spin). Thus, we describe these systems using spin-unrestricted DFT theory. To find the ground-state wave function for each chemisorbed species, we start by estimating the net spin using the IEM (Intersitial Electon Model) model of KG and JMG. For Pt_{35} this is S = 11. Then for this net spin we consider separate self-consistent DFT calculations for all of the low-lying excitations of the higher occupied MOs to the lower unoccupied MOs to ensure that we have found the best orbital occupation for this spin. Afterwards, we consider higher and lower spins by $\Delta S \approx 3$ (e.g., $S = 8-14$ for Pt_{35}) and carry out the same studies to determine the lower lying states for each spin. Consequently, for every adsorbate-cluster system (at each site) we generally calculate ≈20 states, for which we report just the lowest energy case here.

Sometimes DFT calculations for slabs and clusters are carried out for closed-shell configurations in which each orbital is doubly occupied. We caution here that for transition metals this approach is likely to give excited states and unreliable binding sites and energies. For example, the complete closed-shell treatment of the CH_2 chemisorption at the μ_2 bridge site of Pt(111) leads to a binding energy of 133.08 kcal/mol, which is 37.83 kcal/mol higher than obtained using the optimum spins.

It should also be noticed, that for certain systems nearby spin states differ by less than 1 kcal/mol. In these cases, the level of theory is not accurate enough to allow a clear distinction, but a higher level of theory would be needed.

3. Results

3.1. Cluster Model for the Pt(111) Surface. In previous studies,[7] we found that the 12 atom single-layer cluster Pt_{12} leads to a good description for adsorption at the on-top and bridge sites. However, for adsorption at the 3-fold sites, we found that three layers of atoms are required for reliable bond energies. For the adsorption of a single oxygen atom, we found that the three layer model $Pt_{9.10.9}$ (9 atoms in the first and third layers and 10 atoms in the second layer) leads to cluster-size converged results as well as good agreement with calculations on periodic slabs and with experiments on single crystals. Since the high electronegativity of oxygen strongly disturbs the electronic density distribution of the Pt surface, we concluded that the finite cluster that describes accurately the adsorption of atomic oxygen is suitable also for other species.

All calculations presented in this paper are based on the $Pt_{14.13.8}$ cluster (hereafter Pt_{35}). This systems has the advantage over the previous 28 atom $Pt_{9.10.9}$ cluster that the first two layers are slightly larger, minimizing edge effects for more complex adsorbed compounds and surface reactions. Comparing the adsorption of atomic oxygen we find only minor differences in the binding energies obtained with Pt_{28} and Pt_{35}: $\Delta E = 1.91$ (on top), 1.38 (bridge), 1.84 (hcp), and 1.98 kcal/mol (fcc). Since in case of the Pt_{35} cluster we also take care of possible surface relaxation effects (Pt_{28} was completely fixed), the Pt surface is allowed to rearrange under the influence of oxygen, which causes a slightly stronger surface bond for all sites on Pt_{35}. This again confirms that Pt_{28} already leads to cluster-size converged results.

To account for surface relaxation induced by the adsorbate, we allowed the four central atoms of the top layer to fully optimize under the influence of the adsorbate. All other atoms were fixed at the bulk crystal structure with a Pt−Pt distance of 2.775 Å.

As a reference for the adsorbate studies, we calculated the bare cluster Pt_{35}. We find that the positions of the four nonfixed atoms in the first layer changed by less than 3%, indicating negligible relaxation of the Pt(111) surface (This is consistent with experimental observations.[21]).

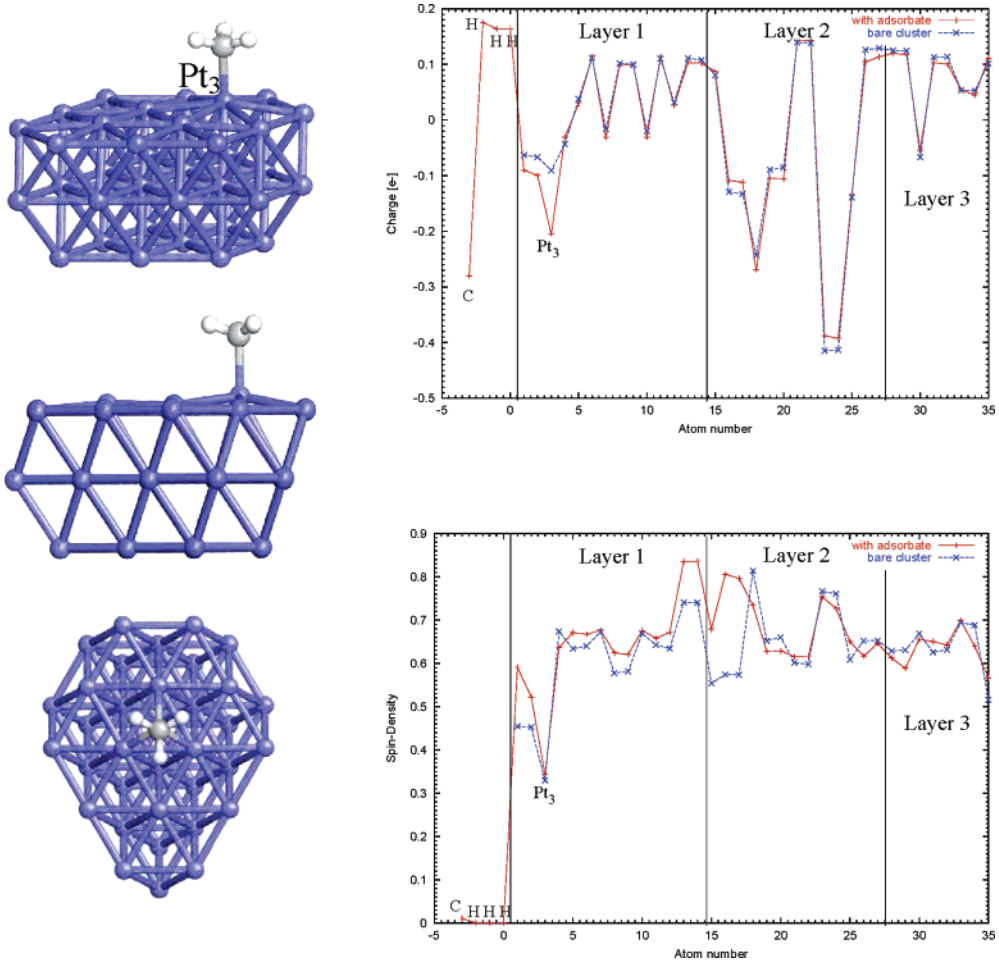

Figure 1. Optimized structure for CH_3/Pt bond on top of a Pt atom. The upper plot on the right side shows the charges and the lower plot the distribution of the spin-density for methyl derived from the Mulliken analysis.

In the interstitial electron model (IEM) for Pt surfaces [based on the IEM model of metal clusters[7,22]] each Pt atom is considered to start with an effective $6s^1 5d^9$ electronic configuration, and then the s-like orbitals are combined into electron pairs localized in alternate tetrahedral interstices [interstitial bond orbital (IBO)]. After subtracting the electron pairs involved in the IBOs, the remaining electrons are distributed among the localized d orbitals. The d orbitals are considered to have smaller overlaps with each other leading to bands for which Hund's rule (maximally allowed spin) provides a good estimate of the net spin. For Pt this leads to a net spin equal to the number of IBOs (or tetrahedron). Since the first and the third layer of bare Pt_{35} represent surfaces, we expect the spin state to be the number of interstitial orbitals (or tetrahedron) formed between the first and second layer plus those between the third and second layer. Assuming the first layer to be the basis plane of each tetrahedra, eight complete tetrahedron are formed between the first two surface layers. This procedure immediately defines the third layer to form the basis plane of tetrahedron between the second and third cluster layer, which then allows 3 complete tetrahedron to be located. Thus, the total number of IBOs is expected to be the sum of all complete tetrahedron, namely 11. Indeed, we find exactly this spin state to be the ground spin-state of the Pt_{35} cluster. Concerning the charge distribution the bare Pt_{35} has a dipole moment of 0.79 Debye (0.31 a.u.).

As initial structures for the geometry optimization of the different adsorbates we started with the adsorbate structures from KG[8] using Pt_8. KG found that every hydrocarbon with a single carbon atom prefers to form four σ-bonds. Consequently, CH_3 binds to the μ_1 site on-top of a Pt atom (Figure 1), CH_2 binds at the μ_2 bridge site (Figure 3 left), and CH (Figure 4 left) adsorbs at the μ_3 3-fold position, as does C. This is consistent with carbon forming four directed bonds expected from sp^3 hybridization. The same conclusion that C generally maintains a tetrahedral configuration was discussed by Papoian et al.[23]

Since many compounds adsorb at the μ_3 site, we expect that our three-layer model will lead to energetics matching the infinite surface much better than the previous one-layer model. In addition, these larger clusters allow us to distinguish between the two different μ_3 (3-fold) sites: (1) hcp, with a second-layer atom located beneath the μ_3 site and (2) fcc, no atom in the second layer beneath the μ_3 site.

For three adsorbates that prefer binding to μ_3 sites (CCH_3/Pt, HCCH/Pt, $CHCH_2$/Pt), we calculated the adsorption at both the hcp and fcc sites. In each case, the adsorption at the fcc site is stronger by 2−7 kcal/mol. Since we are only interested in the most stable structures and energetics, we focused on the adsorption at the fcc site for all other μ_3-bonded systems.

The energetics of the gas-phase adsorbates are summarized in Table 1, and the corresponding energetics and relevant distances of the adsorbed molecules in Tables 2 and 3. For all species except CH_3 and CH_2CH_3, the charge distribution and spin density analysis is given in the Supporting Information (in addiation to the atom numbering used for these plots).

3.2. CH_3 and CH_2CH_3 on Pt(111). *3.2.1. CH_3 (Methyl).* Figure 1 shows the top and side views of CH_3 bound to the Pt(111) plane of the Pt_{35} cluster. The carbon sits directly over the Pt with a bond distance of 2.049 Å (KG: 2.07 Å).

TABLE 1: Total Energies, Ground-State Spins, and Heats of Formation for All Compounds (Gas Phase)

system	total energy [hartree]	spin S	ΔH_f [kcal/mol]
Pt_{35}	−4171.575 47	11	0
CH	−38.477 94	1/2	+152.53
CH_2	−39.150 59	1	+100.21
CH_3	−39.840 54	1/2	+37.03
CH_4	−40.523 24	0	−21.60
CC	−75.879 78	0	+240.78
CC	−75.914 19	1	+219.18
CCH	−76.602 62	1/2	+156.96
CCH_2	−77.261 03	0	+113.57
CCH_3	−77.826 14	1/2	+128.73
C_2H_4	−78.592 02	0	+12.5
HCCH	−77.327 78	0	+71.69
$CHCH_2$	−77.902 99	1/2	+80.51
$CHCH_3$	−78.478 27	1	+89.29
CH_2CH_3	−79.162 05	1/2	+29.98
C_2H_6	−79.837 21	0	−23.91
$C4H_{10}$	−158.467 48	0	−30.03

The adiabatic bond energy for dissociating the CH_3 from the surface is 49.89 kcal/mol (KG: 53.77 kcal/mol). The H−C−H angle is 111.19°, whereas the average Pt−C−H bond angle is 107.7°. As discussed by KFG, the net bond of CH_3 to the surface can be analyzed in terms of a promotion energy of 4.69 kcal/mol to deform gas phase planar CH_3 to the observed bond angle of 111.2° plus a "vertical bond energy" of 49.89 + 4.69 = 54.58 kcal/mol. Such theoretical quantities are useful for estimating chemical processes on surfaces.

Since CH_3 has one unpaired electron available to spin pair (form a covalent bond) with an unpaired d electron of the surface Pt atom, we expect the final ground-state spin to be $S = {}^{21}/_{2}$. However, we find the $S = {}^{23}/_{2}$ state to be 0.33 kcal/mol lower in energy. This indicates that the d σ orbital (perpendicular to the surface) suitable for binding to the CH_3, was weakly spin-paired to a d orbital on some other Pt atom.

All hydrogen atoms in chemisorbed CH_x have a Mulliken charge of +0.17e, whereas the carbon has −0.28e. Thus the net charge transfer from the CH_3 to the cluster is +0.22e, leading to a net dipole moment of 1.18 Debye (0.46 a.u.) for the complex.

3.2.2. CH_2CH_3 (Ethyl). Figure 2 shows the top and side views of ethyl bound to the Pt(111) plane of the Pt_{35} cluster. As shown by KG, we find that ethyl binds to a single Pt atom of the Pt(111) plane. The C_b radical sits directly over the Pt with a bond distance of 2.076 Å (KG: 2.13 Å). The CH_3 sits over one of the fcc sites, and the Pt−C−C angle of 116.4° indicates strain due to steric interactions with the surface (it is 9.7° larger than the Pt−C−H angle in the Pt/CH_3 case). The C_b−C_a bond distance is 1.516 Å, just slightly shorter than the 1.530 Å calculated for free C_2H_6.

The total bond energy to the surface is 46.58 kcal/mol (KG: 45.08 kcal/mol). As for CH_3, we can analyze this in terms of a promotion energy of 4.88 kcal/mol to deform the free CH_2CH_3 to the observed structure of the CH_2CH_3 bound to the surface. This leads to a "vertical bond energy" of 46.58 + 4.88 = 51.46 kcal/mol, which can be compared to the vertical bond energy of 54.58 kcal/mol for CH_3. This difference of 3.12 kcal/mol between the vertical binding energies might be considered as the sum of electronic effects (hyperconjugation) plus steric effects.

The adiabatic bond energy for dissociating the CH_2CH_3 from the surface is 46.58 kcal/mol (KG: 45.08 kcal/mol), which is 3.31 kcal/mol (KG: 8.69 kcal/mol) weaker than from Pt/CH_3. We consider this decrease by 3.3 kcal/mol to be a strain energy due to interaction of the CH_3 with the Pt surface, which influences charge distribution and therefore the electronic structure of the system. This substituent effect is analogous to the difference between the H−CH_3 and H−CH_2CH_3 bonds. Thus, we calculate that the difference between the bond energy for H−CH_3 (calculated to be 114.48 kcal/mol) and H−CH_2-CH_3 (calculated to be 109.75 kcal/mol) is 4.73 kcal/mol, which can be compared to the experimental difference (at 298K) of 104.8 − 101.5 = 3.3 kcal/mol.[24,25]

The chemisorbed system has a ground-state spin of $S = {}^{21}/_{2}$, as expected from spin pairing the radical electron of the ethyl with a localized unpaired d electron of the Pt.

We find that the CH_2 group bound to the surface has a net Mulliken charge of +0.20e (C_b has a charge of −0.13e), whereas the outer CH_3 group has a net charge of +0.12e (C_a has a charge of −0.31e). This leads to a net charge of the adsorbate of +0.32e (which can be compared to +0.22e for the adsorption of CH_3 on Pt). This leads to a net dipole moment for the complex of 2.23 Debye (0.88 a.u.).

The net spin on the ethyl is 0.013, indicating nearly perfect spin pairing to the cluster. The Pt atom to which C_b binds keeps nearly the same spin density of 0.25 as in the free cluster, whereas the two Pt atoms closest to C_a show an increase in spin-density by 0.07 and 0.12.

3.3. CH_2 and $CHCH_3$ on Pt(111). *3.3.1. CH_2 or Methylidene (Methylene).* The left side of Figure 3 shows the top and side views of CH_2 bound to the Pt_{35} cluster. The ground state of free CH_2 is the spin triplet with 2 unpaired spins available for binding to the surface. These bind to the μ_2 bridge site, where both carbon unpaired electrons can spin pair to localized d orbitals on two adjacent surface Pt atoms. This structure has two Pt−C bonds of 2.033 Å (KG: 2.01 Å) with an H−C−H angle of 113.5° and a Pt−C−H angle of 114.3°.

The total bond energy to the surface is 95.26 kcal/mol (KG: 104.28 kcal/mol). This corresponds to an average Pt−C bond of 47.63 kcal/mol, just 2.26 kcal/mol lower than for CH_3, showing bond additivity. The net bond of CH_2 to the surface can be analyzed in terms of a promotion energy of 3.68 kcal/mol to deform the free CH_2 (bond angle of 132.0°) to the observed H−C−H bond angle of 113.5° plus a "vertical bond energy" of 95.26 + 3.68 = 98.94 kcal/mol. We can compare this average vertical bond energy (per Pt−C bond) of 49.47 kcal/mol to the vertical bond energies to the Pt surface of 54.58 kcal/mol for CH_3 and 53.58 kcal/mol for CH_2CH_3.

The nature of the covalent bond is confirmed by the spin-density analysis (see the Supporting Information): chemisorbed CH_2 has nearly no net spin (0.02) and both Pt atoms to which it binds have a drastic reduction in the spin (from 0.45 to 0.22). Moreover, the final chemisorbed ground state spin is $S = 10$, indicating that two unpaired Pt spins are now spin paired. The H has a slightly positive Mulliken charge of +0.19e, whereas the carbon has −0.20e, resulting in a net charge transfer from the CH_2 to the cluster of +0.18e. This leads to a cluster dipole moment of 1.62 Debye (0.64 a.u.).

3.3.2. $CHCH_3$ (Ethylidene). Replacing one H of CH_2 with CH_3 leads to ethylidene, which also binds to the μ_2 bridge site (Figure 3 right) with a Pt−C_a bond length of 2.048 Å as compared to 2.033 Å for Pt−CH_2. The C_a−C_b bond is 1.501 Å, or 0.030 Å longer than for the free ethylidene but 0.029 Å shorter than calculated for C_2H_6.

When two covalent bonds to the surface are formed, we expect the ground-state spin to change from $S = 11$ to 10. However, this state is 0.10 kcal/mol higher than the $S = 11$ state, indicating that bonding has unpaired a spin pair between two surface d orbitals. Again, the net spin density of the adsorbate is nearly zero (0.02) and the spin density on the two

TABLE 2: Binding Characteristics of the Adsorbed CH_x Species[a]

system on Pt_{35}	total energy [hartree]	spin S	bind. energy [kcal/mol]	distances [Å]	angles [deg]	ΔH_f [kcal/mol]
C	−4209.654 30	10	−147.87	$Pt_{1/2/3}-C = 1.870$		+33.20
CH	−4210.287 05	21/2	−146.61	$Pt_{1/2/3}-C = 1.981$ $C-H = 1.091$	$S_\perp$-CH = 1.4 $Pt_{1/2}-C-H = 131.2$ $Pt_3-C-H = 133.8$	+5.92
CH_2	−4210.877 86	10	−95.26	$Pt_{1/2}-C = 2.033$ $C-H = 1.091$	$S_\perp$-CH_2 = 0.7 $H-C-H = 113.5$ $Pt_1-C-Pt_2 = 82.3$	+4.95
CH_3	−4211.495 53	23/2	−49.89	$Pt_3-C = 2.049$ $C-H = 1.092$	$S_\perp$-CH_3 = 0.6 $H-C-H = 111.2$ $Pt_3-C-H = 107.3$ (2×) $Pt_3-C-H = 108.5$ (1×)	−12.87
	−4211.495 00	21/2	−49.56	(see $S = {}^{23}/_2$)	(see $S = {}^{23}/_2$)	−12.54

[a] $S_\perp$ denotes the surface normal vector.

TABLE 3: Binding Characteristics of the Adsorbed C_2H_y Species[a]

system on Pt_{35}	total energy [hartree]	spin S	bind. energy [kcal/mol]	distances [Å]	angles [deg]	ΔH_f [kcal/mol]
CC	−4247.679 38	10	−140.64	$Pt_{1/2}-C_a = 1.977$ $Pt_3-C_a = 2.196$ $Pt_3-C_b = 2.013$ $C_a-C_b = 1.360$ $S_{\|\|}-Pt_3 = 0.796$	$S_\perp-CC = 42.6$ $(Pt_1\text{-}C_a\text{-}Pt_2)-CC = 19.2$	+100.13
CCH	−4247.679 38	9	−140.64	(see S = 10)	(see S = 10)	+100.13
	−4248.976 60	21/2	−99.49	$Pt_{1/2}-C_a = 2.000$ $Pt_3-C_a = 2.218$ $Pt_3-C_b = 1.993$ $C_a-C_b = 1.323$ $S_{\|\|}-Pt_3 = 0.891$	$S_\perp-CC = 43.3$ $(Pt_1\text{-}C_a\text{-}Pt_2)-CC = 20.3$ $C_a-C_b-H = 146.0$	+57.46
	−4248.335 66	19/2	−98.88	(see $S = {}^{21}/_2$)	(see $S = {}^{21}/_2$)	+58.08
CCH_2	−4248.976 60	10	−87.92	$Pt_{1/2}-C_a = 1.968$ $Pt_3-C_a = 2.114$ $Pt_3-C_b = 2.278$ $C_a-C_b = 1.393$ $S_{\|\|}-Pt_{1/2} = 0.372$ $S_{\|\|}-Pt_3 = 0.448$	$S_\perp$-CC = 40.8 $(Pt_1\text{-}C_a\text{-}Pt_2)-CC = 14.1$ $(H\text{-}C_b\text{-}H)-CC = 16.3$	+25.65
CCH_3	−4249.616 47	21/2	−134.83	$Pt_{1/2/3}-C_a = 1.997$ $C_a-C_b = 1.489$ $C_b-H = 1.097$	$S_\perp-CC = 2.4$ $C_a-C_b-H = 110.3$ $H-C_b-H = 108.7$ $Pt_{1/2}-C_a-C_b = 124.5$ $Pt_3-C_a-C_b = 125.5$	−6.10
	−4249.615 90	19/2	−134.47	(see $S = {}^{21}/_2$)	(see $S = {}^{21}/_2$)	−5.74
di-σ-C_2H_4	−4250.209 63	10	−26.44	$Pt_{1/2}-C_{a/b} = 2.100$ $C_a-C_b = 1.494$ $C-H = 1.092$	$S_\perp-C_2H_4 = 0.6$ $Pt_{1/2}-C_{a/b}-H = 103.5$ $H-C-H = 112.7$ $(H\text{-}C\text{-}H)-(C_a\text{-}C_b) = 41.3$	−8.54
π-C_2H_4	−4250.184 37	11	−10.59	$Pt-(C{=}C) = 2.081$ $C_a-C_b = 1.407$ $S_{\|\|}$-Pt_3 = 0.513	$H-C-H = 116.1$ $C-C-H = 120.2$ $(H\text{-}C\text{-}H)-CC = 18.5$	+7.31
HCCH	−4248.973 24	10	−43.91	$Pt_{1/2}-C_{a/b} = 1.987$ $Pt_3-C_{a/b} = 2.225$ $C_a-C_b = 1.389$ $S_{\|\|}-Pt_3 = 0.445$	$S_\perp-HCCH = 27.2$ $H-C_a-C_b = 126.3$ $Pt_{1/2}-C_{a/b}-H = 121.2$ $Pt_1-C_a-C_b-H = 170.6$	+27.76
$CHCH_2$	−4249.594 18	19/2	−72.62	$Pt_3-C_a = 2.078$ $Pt_{1/2}-C_b = 2.047$ $C_a-C_b = 1.476$	$S_\perp-CC = 75.1$ $H-C_b-C_a = 121.2$ $H-C_a-C_b = 114.7$	+7.89
	−4249.592 06	21/2	−71.28	(see $S = {}^{19}/_2$)	(see $S = {}^{19}/_2$)	+9.22
$CHCH_3$	−4250.197 54	11	−90.24	$Pt_{1/2}-C_a = 2.048$ $C_a-C_b = 1.501$ $S_{\|\|}-Pt_{1/2} = 0.503$	$S_\perp-(Pt_1\text{-}C_a\text{-}Pt_2) = 4.0$ $S_\perp-CC = 41.2$ $H1-C_a-C_b = 110.9$ $C_b-C_a-H_2 = 114.1$ $C_b-C_a-H_{3/4} = 108.7$	−0.96
CH_2CH_3	−4250.197 40	10 21/2	−90.14	(see S = 11)	(see S = 11)	−0.86
	−4250.811 76		−46.58	$Pt_3-C_b = 2.076$ $C_a-C_b = 1.516$	$S_\perp-C_b = 61.4$ $S_\perp-C_b = 2.7$	−16.61
	−4250.811 41	23/2	−46.36	(see $S = {}^{21}/_2$)	−	−16.39

[a] $S_\perp$ denotes the surface normal vector.

Pt bonded to the adsorbate decrease from 0.45 to 0.27 upon binding (see supporting material).

The net charge on the CH_3 is +0.16e (with −0.30e on the C b), whereas the charge on the CH is +0.11e (with −0.08e on the C a). Thus, the total charge is +0.27e on the organic and −0.14e on the two Pt bound to it. This leads to a cluster dipole moment of 2.60 Debye (1.02 au).

The total bond energy to the surface is 90.24 kcal/mol (KG: 98.05 kcal/mol), which is 5.02 kcal/mol weaker than for CH_2/Pt. This can be considered partly as a substituent effect. Thus, removing two H atoms from CH_4 costs 233.51 kcal/mol while removing two H atoms from the same C of C_2H_6 costs 224.91 kcal/mol, a difference of 11.40 kcal/mol or over twice the value for Pt surface.

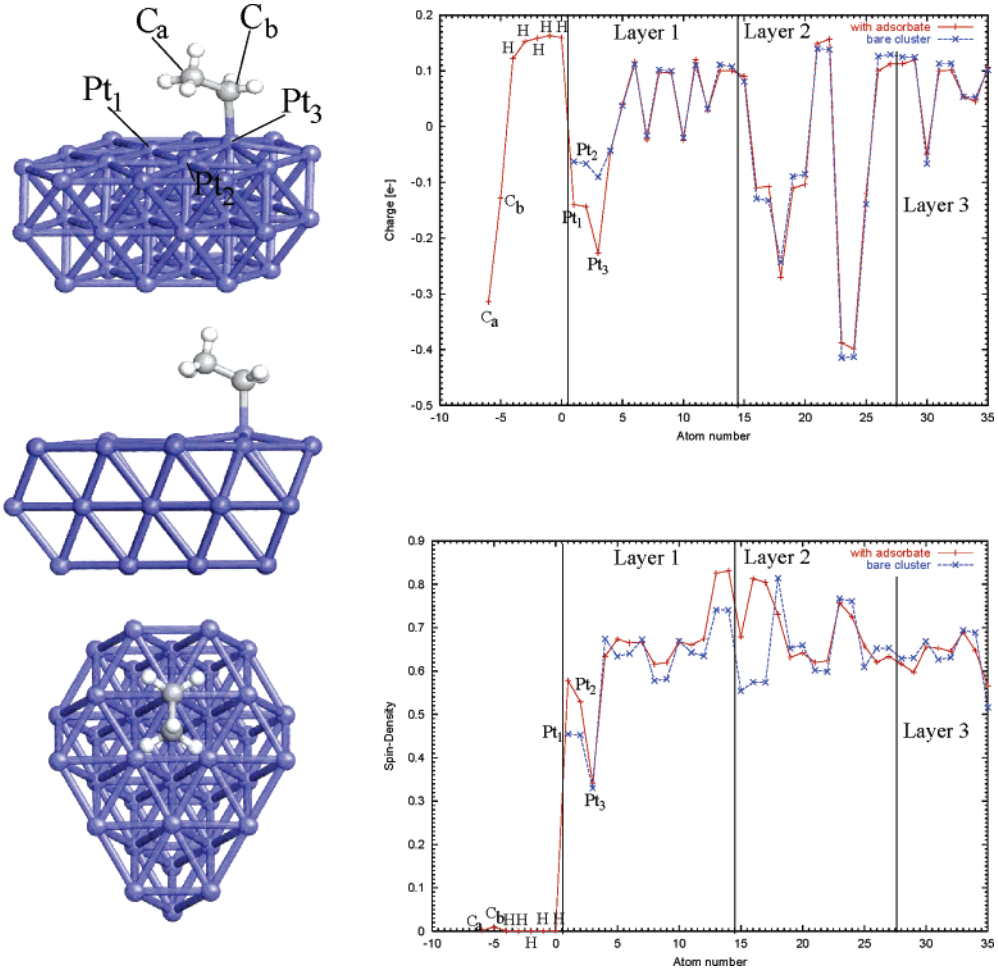

Figure 2. Optimized structure for CH_2CH_3/Pt, leading to an μ_1 (or on-top) site with the CH_3 group lying over the adjacent hcp site. The upper plot on the right side shows the charges and the lower plot the distribution of the spin-density for ethyl derived from the Mulliken analysis.

For this system, the calculation of snap bond energy is a bit more complicated. At the B3LYP level, free $CHCH_3$ has a triplet ground state (H−C−C = 132.11°) with the singlet state (H−C−C = 104.25°) 6.65 kcal/mol higher. Promoting the free triplet $CHCH_3$ to the structure of bound $CHCH_3$ costs 5.81 kcal/mol. Adding this to the adiabatic bond energy leads to a snap bond energy of 90.24+5.81 = 96.05 kcal/mol, which can be compared to the value of 98.94 kcal/mol for CH_2.

3.4. CH and CCH_3 on Pt(111). *3.4.1. CH (Methylidyne).* Figure 4 shows the top and side views of CH bound to the Pt(111) plane of the Pt_{35} cluster. KG showed that CH makes the best bond to the μ_3 triangle site, where the three carbon electrons not binding to H can spin pair with localized d orbitals on the three surface Pt atoms, leading to three equivalent bonds. We find the same result and moreover confirm that the bond to the fcc site is 5.78 kcal/mol stronger than to the hcp site (as expected by the IEM).

The optimum geometry has three Pt−C bonds of 1.981 Å (KG: 1.95 Å), which are 0.052 Å smaller than for CH_2 and 0.068 Å smaller than for CH_3. The CH bond is perpendicular to the surface, leading to a Pt−C−H angle of 123.58°.

The nature of the bond is confirmed by the spin-density analysis (see supporting material): chemisorbed CH has nearly no net spin (0.03) and two of the Pt atoms to which it binds reduce their spin from 0.45 to 0.29, whereas the third Pt atom reduces its net spin from 0.33 to 0.28. Thus, despite a cluster symmetry that leads to inequivalent Pt, the bonded system has three nearly equivalent Pt. In addition, the third-layer atom beneath the adsorbate reduces its spin significantly (from 0.67 to 0.46). All other Pt atoms show little change in net spin.

The charge on the H is +0.18e, whereas the C has a charge of −0.18e. Thus, there is almost no net charge transfer to the surface. This leads to a cluster dipole moment of 1.21 Debye (0.48 a.u.).

The binding energy of CH to the surface is 146.65 kcal/mol or 48.88 kcal/mol per Pt−C bond. This can be compared to an energy of 47.63 kcal/mol per Pt−C bond for CH_2, and 49.89 kcal/mol for CH_3. Thus, one can consider every Pt−C bond to add ≈48.8 kcal/mol (average value).

The ground state of free CH is the $^2\Pi$ state with one unpaired p-π orbital, a doubly occupied σ orbital, and an empty p-π orbital. To obtain the three unpaired spins to bind to the 3 Pt of the μ_3 site, we consider that the CH is promoted to the $^4\Sigma^-$-state (19.40 kcal/mol higher in B3LYP) with three singly occupied orbitals (one σ and two π). Thus, with respect to this promoted state the net binding is 166.05 kcal/mol.

However, the net reduction in the ground-state spin is $\Delta S = {}^1/_2$. This is consistent with binding to the ground state of CH (the $^2\Pi$ state), rather than the $^4\Sigma^-$ state that has three unpaired spins. Exactly the same result was obtained by KG, and as discussed there, this suggests that our analysis is a bit oversimplified.

3.4.2. CCH_3 (Ethylidyne). The structure of chemisorbed ethylidyne (Figure 4) is equivalent to ethane. Each C atom shows sp^3 hybridization with C_a forming three covalent bonds to the surface (1.997 Å). The C_a−C_b bond distance is 1.489 Å, indica-

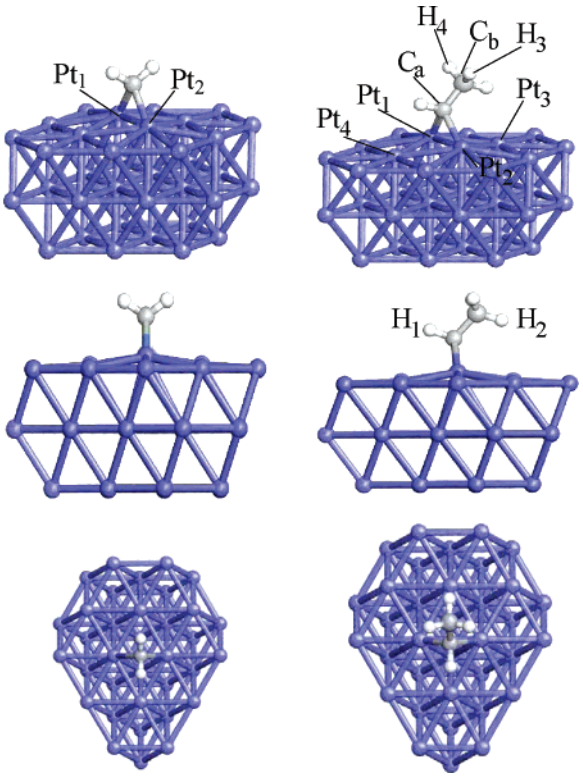

Figure 3. Optimized structures for CH_2/Pt, binding to an μ_2 or bridge site, and $CHCH_3$/Pt also leading to an μ_2 or bridge site, but with the CH_3 group lying over the adjacent hcp site.

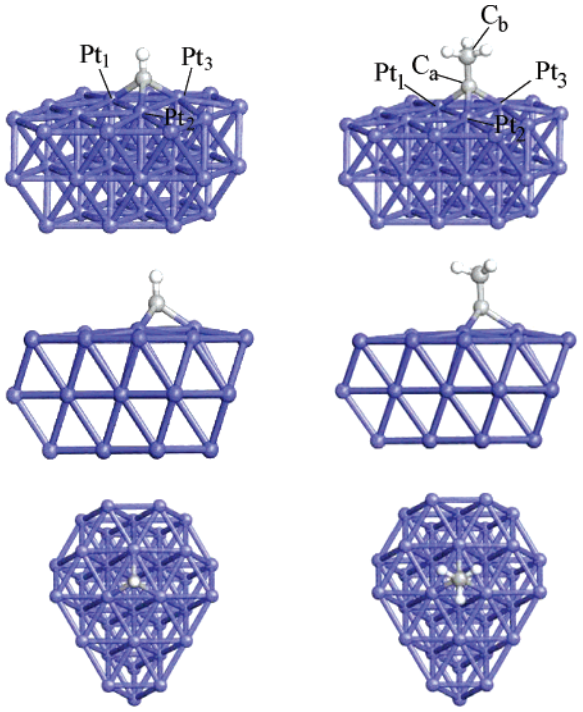

Figure 4. Optimized structure for CH/Pt, binding to an μ_3 site, and CCH_3/Pt, leading to an μ_3 site with the CH bonds over the adjacent hcp sites.

ting a single bond. The calculated C−C bond distance can be compared to 1.530 Å for free C_2H_6, 1.516 Å for CH_2CH_3, and 1.501 Å for $CHCH_3$. We interpret this as indicating that the intrinsic C−C single bond is close to 1.49 Å, with replacement of each Pt by a H increasing the C−C bond distance by 0.01 to 0.02 Å due to steric (Pauli repulsion) interactions with the CH_3

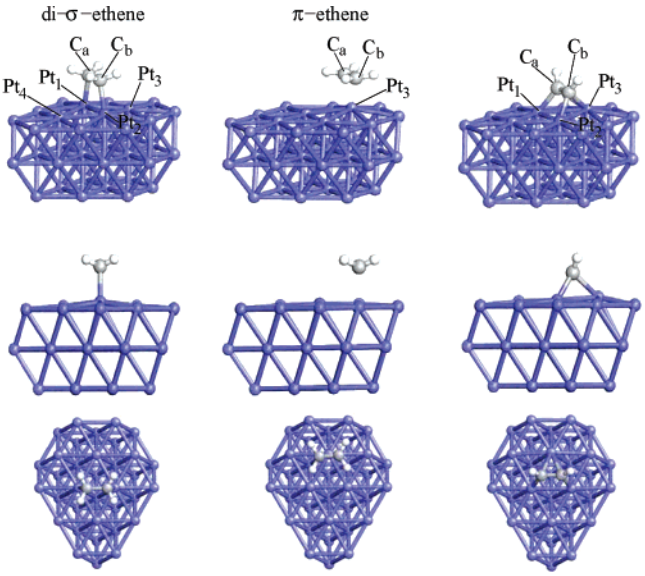

Figure 5. Optimized structure for ethene (C_2H_4/Pt) and acetylene (HCCH/Pt). Among the C_2H_4 species the di-σ state is most stable with bonds to an μ_2 site. To obtain the π-ethene structure, it was necessary to constrain the C−C bond midpoint to lie over a Pt.

(which is weaker than for Pt). This is consistent with the 1.47 Å bond calculated for ethylene twisted by 90 degrees.[26]

The charge on the outer CH_3 is +0.17e (C b: −0.34e), whereas C_a has a charge of −0.10e. Thus, the net charge transfer to the surface is +0.07e, and the Pt cluster shows only minor charge displacements (see the Supporting Information). The total cluster dipole moment is 2.35 Debye (0.93 a.u.).

Chemisorption of CH changes the ground-state spin from $S = 11$ of the bare cluster to $S = {}^{21}/_{2}$. Just as for CH, only two of the surface Pt atoms have a significant reduction in their net spin upon CCH_3 chemisorption (from 0.45 to 0.29), but the net spin on the adsorbate is only 0.03. In addition, the second-layer Pt atoms that are beneath the adsorption site show larger changes in the net spin.

The net bond energy of CCH_3 to the surface is 134.83 kcal/mol, which is 11.82 kcal/mol weaker than for CH. Since the CH_3 points away from the surface, it is not plausible that this can be interpreted as a steric effect involving interaction with the surface. Instead, we consider analyze the binding of CH and CCH_3 in terms of the promotion of the $^2\Pi$ ground state to the $^4\Sigma^-$ state, having the three unpaired spins required to bond to the three Pt atoms of the surface. This promotion energy is 19.40 kcal/mol for CH and 32.96 kcal/mol for CCH_3. This model suggests that the net bond energy for CCH_3 to the surface would be

$$146.65\ (\text{CH/Pt adsorp. energy}) + 19.40\ (\text{CH promotion})$$
$$- 32.96\ (\text{CCH}_3\ \text{promotion}) = 133.05\ \text{kcal/mol}$$

which agrees with the QM value 134.83 kcal/mol.

The same promotion analysis can be more for the carbon species. Thus, starting with CH_4 and C_2H_6 and removing all three H from one carbon leads to a calculated total bond energy of 320.20 kcal/mol and 341.68 kcal/mol, respectively, which differ by 21.45 kcal/mol in the same order with the differential promotion energy of 13.56 kcal/mol obtained from previous analysis on the surface.

3.5. Ethene (Ethylene) and Ethyne (Acetylene). *3.5.1. CH_2CH_2 or Ethene (Ethylene).* We find that ethene (see Figure 5) adsorbs on the Pt(111) surface by binding to an μ_2 bridge

site with covalent single bonds to each of the two Pt atoms, leading to the di-σ-bonded state with Pt−C bonds of 2.100 Å (KG: 2.06 Å). Thus, each C has the binding expected of sp^3-hybridized orbitals. Here the C−C bond is 1.494 Å, indicating a σ bond. The CH_2 group is bent away from the C−C bond by 41.3° and the Pt−C−H angle is 103.5°.

The net spin of the system decreases by $\Delta S = 1$ to 10 as expected for forming two covalent bonds. Again, there is essentially no net spin (0.02) on the adsorbate (every electron is spin paired), and the only significant reductions in spin (from 0.45 to 0.20) are for the two Pt atoms to which bound to the adsorbate.

The net charge on the di-σ ethene is +0.44e (with a charge of −0.15e on each C and +0.19e on each H), whereas the two bonded Pt have charges of −0.21 and −0.23e. This leads to a cluster dipole moment of 2.77 Debye (1.09 a.u.).

We calculate that the net bond relative to free ethene is 26.44 kcal/mol (KG: 36.05 kcal/mol). This bond strength can be analyzed as follows. The bond energy of ethyl to Pt(111) is 46.58 kcal/mol but we have to break the π bond of ethene, which can considered as ≈65.92 kcal/mol (obtained from QM calculations on the process of converting ethane to ethene). Thus

$$\text{DH(di-}\sigma\text{ ethene)} = (\pi\text{-bond of ethene}) - 2 \times \text{BE(ethyl/Pt)}$$
$$= 65.92 - 2 \times 46.58 = -27.24 \text{ kcal/mol}$$

which is in very good agreement to the QM calculation, and analogous calculations by KG

$$\text{DH(di-}\sigma\text{ ethene)} = 65.92 - 2 \times 45.08 = -24.24 \text{ kcal/mol}$$

compared to their QM value of 36.05 kcal/mol. This suggests that the bond additivities are not as good for the one-layer clusters, perhaps because the surface electrons can repolarize better for each bonding case.

In addition to the di-σ bonding found for the ground state, it is useful to know the energy of the state in which the C═C π bond is not broken. To find this state, we restricted the center of the C−C bond to lie directly above a Pt, and stabilized a second state in which the C═C π bond is not broken (the structure was fully optimized except for this constraint). This π-ethene leads to a net bond energy of 10.59 kcal/mol (15.85 kcal/mol weaker than di-σ) with C−C = 1.407 Å and Pt−C = 2.081 Å. Minimizing from this π-bound ethene, leads to the di-σ state with no energetic barrier.

We found no change in the net spin for π-ethene, indicating that it has not bonded to the Pt d-orbitals. Thus, the structure is bonded to the surface as a donor−acceptor bond via the π orbital of the C═C double bond. The net charge on the π-ethene is +0.48e (with a charge of −0.12e on each C), whereas the bonded Pt has a charge of −0.32e. This leads to a cluster dipole moment of 3.81 Debye (1.46 a.u.).

3.5.2. HCCH or Ethyne (Acetylene). We find that ethyne adsorbs at the μ_3 fcc site (Figure 5) with each C atom forming one covalent σ-bond to a surface atom (Pt−$C_{a/b}$ = 1.987 Å). (The binding to this site is 2.89 kcal/mol better than binding to the hcp site.) However, these bonds are bent to an angle of 27.2° from the normal, so that each C is 2.225 Å from the third Pt. The C−C bond increases from 1.205 Å in free ethyne to 1.389 Å, indicating a double bond comparable to the π complex of ethene (1.407 Å) and to free ethene (1.332 Å). We interpret this third bond as a donor−acceptor π bond. Thus, HCCH binds on the surface like ethene, but with an additional donor−acceptor (DA) π bond. This (di-σ/DA-π) bond model of binding was also found by KG, where the Pt−C bonds were 1.94 Å (twice) and 2.12 Å.

This model of binding is also confirmed by the spin-density analysis, which finds a reduction by 0.14 for the nearest two Pt atoms, but nearly no change (0.02) for the third Pt of the fcc-triangle. The net result is a reduction of the ground-state spin by $\Delta S = 1$ due to the adsorbate (from $S = 11$ for the bare cluster to $S = 10$ for the cluster+adsorbate system).

As for nearly all other hydrocarbons, there is no net spin on the adsorbate (total of 0.08). However, the net charge on the HCCH is +0.22e (−0.09e on each C), whereas the three Pt atoms have charges of −0.12e (twice) and −0.19e (the DA-π bond). This leads to a cluster dipole moment of 2.82 Debye (1.11 a.u.).

The net bond energy relative to free ethyne is 43.91 kcal/mol (KG: 78.83 kcal/mol). To estimate the strength the DA-π bond we use the following analysis. The bond energy to Pt-(111) is 43.91 kcal/mol, but we have to break the π bond of ethyne. To estimate this energy cost, we carried out QM calculations on the process of converting ethene to ethyne. Thus, the energy change for 2H + ethyne → ethene is calculated as 165.48 kcal/mol whereas the H−$CHCH_2$ bond energy is 118.45 kcal/mol. Comparing these two values leads to an energy of 71.43 kcal/mol for breaking the first π-bond of ethyne (2 × 118.45−165.48 = 71.43 kcal/mol). Thus, we calculate that the DA-π bond is 22.2 kcal/mol from the following:

$$\text{DH[(di-}\sigma\text{/DA-}\pi\text{)-ethyne]} = (\pi\text{-bond of ethyne}) - 2 \times \text{BE(ethyl/Pt)} - (\text{DA-}\pi) \Leftrightarrow (\text{DA-}\pi) = -1\cdot(-43.91 + 2 \times 46.58 - 71.43 = +22.18 \text{ kcal/mol.}$$

3.6. Other Hydrocarbons. *3.6.1. $CHCH_2$ (Vinyl).* We find that vinyl ($CHCH_2$) binds to an fcc μ_3 site with two Pt−C_b σ-bonds of 2.047 Å and one Pt−C_a σ-bond of 2.078 Å. The C−C distance is 1.476 Å compared to 1.309 Å for free vinyl (Figure 3). Thus, each C has four bonds as expected for a sp^3-configuration, whereas C_a−C_b is a single bond.

The ground-state spin of the vinyl + cluster is $S = {}^{19}/_2$, as expected for forming three covalent bonds to Pt atoms. The net spin of the vinyl is nearly zero (0.03), and the reduction of spin-density of the two Pt atoms C_b binds to is 0.23. The Pt atom to which C_a binds reduces its net spin by only 0.03.

The net charge on the vinyl is +0.33e (+0.13e on the CH and +0.20e on the CH_2), with charges on each hydrogen of +0.19e. This leads to a cluster dipole moment of 3.00 Debye (1.18 a.u.).

3.6.2. CCH_2 (Vinylidene). The ground state of vinylidene has a π bond from C_a to CH_2 with a doubly occupied s-orbital on C_a (see Figure 3). The triplet excited state of gas-phase CCH_2 (47.25 kcal/mol higher using B3LYP) has one s electron promoted to the empty p orbital on the C_a parallel to the plane. The binding to the surface can be thought of as spin-pairing these two triplet electrons to two adjacent Pt atoms, as in CH_2. This would lead to a structure, in which the C−C bond is perpendicular to the surface. Instead the molecule bends by ≈38° (so that the π bond can interact (DA-π) with the third Pt of an μ_3 site, denoted Pt_3. Here the C_a−Pt_3 and C_b−Pt_3 bonds are 2.114 Å and 2.278 Å, whereas the C_a−Pt_1 and C_a−Pt_2 bonds are both 1.968 Å.

This geometry is comparable to CCH/Pt. However, the binding is completely different. The π orbital of the C═C double bond is perpendicular to the Pt_1−C_a−Pt_2 plane and therefore rotated by 90° compared to the π orbital of CCH/Pt (compare

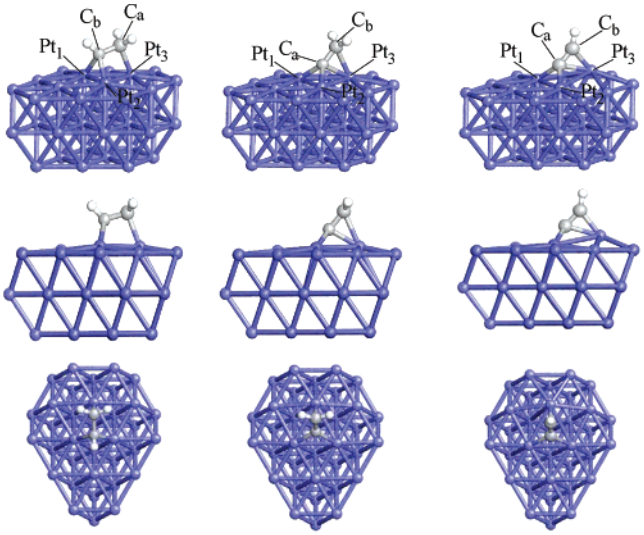

Figure 6. Optimized structures for $CHCH_2$/Pt (vinyl), CCH_2/Pt (vinylidene), and CCH/Pt (ethynyl), which all bind asymmetrically to an μ_3 site.

orbitals shown in Figure 7). This allows the adsorbate to form two covalent bonds to the adjacent Pt atoms ($d = 1.968$ Å).

The significant difference with respect to CCH/Pt is also shown in the spin-density analysis (see supporting material). Compared to ethynyl, CCH_2 causes much less changes in the spin-density of the cluster due to adsorption.

The ground-state spin of the vinylidene/Pt cluster is $S = 10$, as expected for forming two covalent bonds to Pt atoms. The net spin of the vinylidene is only 0.12, and the reduction of spin-density of the two Pt atoms C_a binds to is 0.12 per Pt. The Pt atom to which C_b binds increases its net spin by 0.16.

The net charge on the vinylidene is +0.17e (−0.12e on C_a and +0.29e on the CH_2), with charges on each hydrogen of +0.18e. This leads to a cluster dipole moment of 2.23 Debye (0.88 a.u.).

3.6.3. CCH (Ethynyl). Removing one H from HCCH leads to CCH ($^2\Sigma^+$), which has two C−C π bonds (denoted as π_x and π_y with the C−C axis considered as z) plus a singly occupied σ electron on C_a. One mode of binding to the surface is for the σ orbital to bind on-top of one Pt, leading to a structure in which the CCH is perpendicular to the surface. However, we find a quite different structure in which the CCH bond is bent by ≈43° from the normal. We might expect that the σ-bonded state would bend over so that the π orbitals could make DA bonds to the other two Pt of an μ_3 site, but we find that this state is not the best.

The calculated optimum structure is shown in Figure 6 and the orbitals analyzed in Figure 7 (right). This geometry can be rationalized in terms of the electronic excited state ($^2\Pi$) of CCH in which one π electron is excited to the singly occupied σ orbital. With B3LYP, this state is 5.35 kcal/mol higher than $^2\Sigma^+$. The orbitals of this excited state are consistent with the σ pair inserting between the Pt_1 and Pt_2 atoms to form a bridge bond (the bond distances are 2.000 Å), whereas the singly occupied p-orbital spin pairs to a d-orbital on Pt_3 to form a covalent bond (C_a−Pt_3 = 2.218 Å and C_b−Pt_3 = 1.993 Å).

We found it difficult to analyze the binding for CCH/Pt because the orbitals were too delocalized. Consequently, we carried out a Pipek-Mezey localization of the occupied orbitals for Pt_3−CCH, leading to orbitals shown on the right side of Figure 7. Orbital (c) shows a double bond between C_a and C_b, but with the π bond parallel to the surface. Instead of forming covalent bonds between C_a and the Pt_1 and Pt_2 surface atoms, we find a doubly occupied lone pair (orbital (e)) on C_a directed between both Pt atoms. Only C_b forms one covalent bond to the surface (orbital (d)).

The net charge on the CCH is +0.02e, with −0.11e on C_a, −0.07e on C_b, and +0.21e on H. Thus, for CCH/Pt, all the positive charge originally located on C_b moves to the hydrogen after adsorption. This leads to a cluster dipole moment of 2.00 Debye (0.79 a.u.).

Compared to the bare cluster, the ground-state spin changes by $\Delta S = {}^1/_2$, but the binding energy of the adsorbate is only 0.61 kcal/mol stronger than the state that changes by $\Delta S = {}^3/_2$. The net spin of the CCH is 0.22, with a net spin of 0.16 on C_b and 0.06 on C_a. The spin-density of the Pt atoms bonded to C_a reduces to 0.01, while the Pt atom to which C_b binds reduces its net spin by only 0.05.

3.6.4. Atomic C. Figure 8 shows on the left side the top and side views of a C atom bound to the Pt(111) plane of the Pt_{35} cluster. It binds to an fcc μ_3 site, just as does CH. The bonds to the three nearest Pt atoms are equivalent with a distance of 1.870 Å leading to a net perpendicular distance from the surface of 1.02 Å, which is 0.42 Å smaller than for CH/Pt.

The ground-state spin for C/Pt is $S = 10$, so that binding to the free cluster reduces the spin by $\Delta S = 1$. The analysis of the spin density before and after adsorption (see supporting material) shows a net spin on the adsorbate of only 0.04.

Since the ground state of atomic carbon is a triplet (two singly occupied p orbitals plus the 2s lone pair), the simplest model of binding would have suggested that binding C to the surface would reduce the spin by $\Delta S = 1$, which is observed. Spin pairing the two p orbitals of carbon to the surface would leads to the μ_2 bridge site. Since this site would lead to an empty p orbital parallel to the surface, it is plausible that it might bend around to accept some electrons from the adjacent Pt of the μ_3 site, an donor−acceptor bond in which the adsorbate is the acceptor. This would lead to the 2s lone pair hybridizing and pointing away from the surface. In this description, we would expect that the three bonds, two covalent and one DA, would resonate, leading to three equivalent bonds. To check this description Figure 8 also includes the orbitals obtained after localization. Indeed, orbital (a) corresponds to the C lone pair, whereas (b)−(d) are the three equivalent bonds after resonance. Since the fcc-triangle is broad enough, the distance to the surface is only 0.56 Å and the 2s lone pair remains s-like, pointing very little away from the surface.

An alternative way to think about the binding of C/Pt is as dehydrogenation of CH/Pt: Starting with the CH/Pt, we break the CH bond to leave behind a singly occupied σ orbital pointing at the virtual H position. This would lead to a net spin on the carbon. Leaving this orbital unpaired, the net effect would be to increase the spin of CH/Pt from $S = {}^{21}/_2$ to 11, which is not observed. An alternative here would be for the surface to transfer an electron to the singly occupied orbital, but this would lead to a net negative charge on the C. However, we find a net charge of only −0.11e on the C of the adsorbate compared to −0.18e for the carbon in CH/Pt.

Thus, we conclude that the bond of C in C/Pt should be thought of as a carbon atom forming two covalent bonds plus a donor acceptor bond with the three Pt atoms of an μ_3 site. We find that the net spin of Pt_1 and Pt_2 reduces by 0.22 but that the spin on the Pt_3 atom reduces by only 0.12. This is consistent with the C atom model described in the previous paragraph. In addition, the charge distribution is also consistent with this behavior. The Pt_3 has a net change in charge of +0.13e,

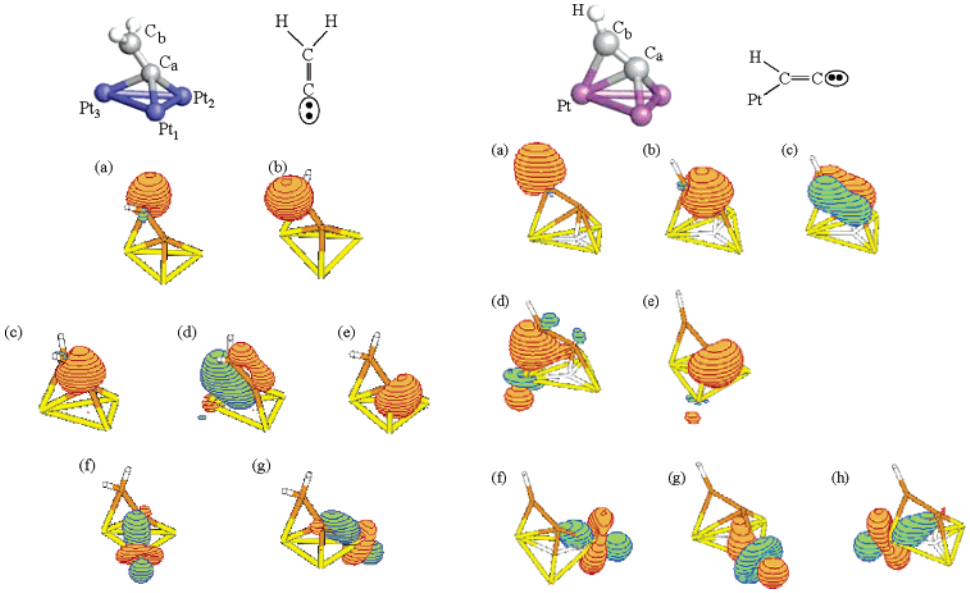

Figure 7. Analysis of the occupied orbitals of the systems Pt_3-CCH_2 and Pt_3-CCH. These orbitals were obtained from a Pipek-Mezey localization.

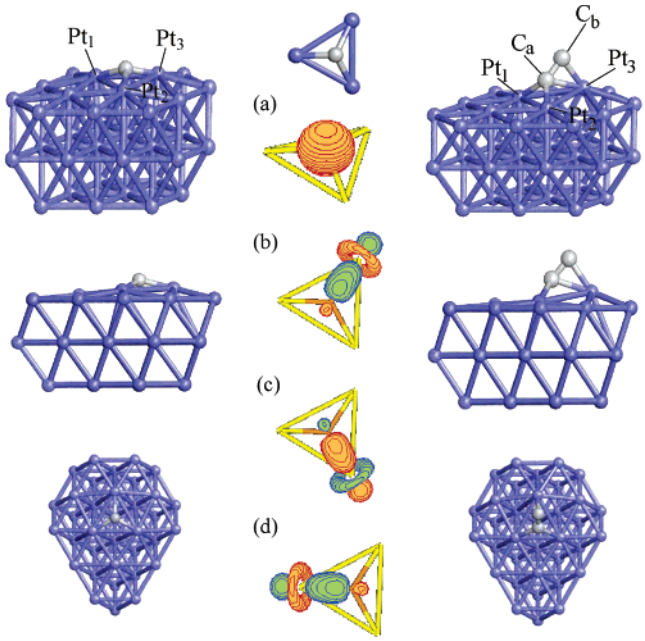

Figure 8. Optimized structures for C/Pt and CC/Pt, which both bind to an μ_3 site. In addition, occupied orbitals of Pt_3-C are analyzed after a Pipek-Mezey localization.

whereas the other two Pt atoms have charge changes of +0.07e. For this case, we observe that the third-layer Pt atom located beneath the adsorbate (labeled Pt_{30}) has its net spin reduced by 0.26. This might result from the donor−acceptor bond, which would polarize a doubly occupied d orbital of Pt_3 toward the C, causing the unpaired d orbital on Pt_3 to make more of a bond to the second layer Pt, resulting in an increased spin on the third lower atom. Alternatively, this might be interpreted as charge transfer to the C unpaired orbital in the dehydrogenation model.

The total bond strength of C and CH to the surface are essentially the same (147.9 versus 146.6 kcal/mol). This indicates that the C−H bond energy of CH/Pt is the same as for free CH, which is 84.39 kcal/mol.

3.6.5. CC. The bonds between C_a-C_b and $Pt-C_a$ of dicarbon (Figure 8 right) lead to a structure with the C−C bond tilted 42.6° from the surface normal. The structure is very much like CCH/Pt, but with the H removed. Indeed the surface bond lengths are essentially unchanged (the two $Pt_{1/2}-C_a$ bonds decrease by 0.025 Å and Pt_3-C_a by 0.022 Å, whereas the Pt_3-C_b bond increases by 0.021 Å). The double bond between C_a- and C_b (1.360 Å) increases by 0.037 Å. The surface Pt_3, located beneath C_b, is lifted up by ≈0.80 Å, which compares to 0.89 Å for CCH/Pt.

The small changes in the structure from CCH to CC suggest that we must consider the structure of CC/Pt to be formed from CCH/Pt by removing the H and leaving behind the unpaired spin on the outer carbon, C_b. This view is supported by the observation that the total energy is the same (differing by less than 0.01 kcal/mol) for two different spin-states: $S = 10$ and 9 (compared to $S = {}^{19}/_2$ for CCH). However, the analysis of the spin-density shows very little net spin on the dicarbon (0.04 on C_a and 0.08 on C_b).

The net charge on the CC is −0.02e, with −0.21e on C_a and +0.19e on C_b, leading to a cluster dipole moment of 2.53 Debye (1.00 a.u.). The only Pt atoms with significant charge change are Pt_2 and both second-layer Pt atoms located beneath the adsorption site (see the Supporting Information).

4. Comparison with Experiment

Although there is some experimental data on kinetics, barriers, and spectroscopy of the CH_x and C_2H_y species,[27] there is still little experimental data on energetics or structures available for comparison to our calculations. To facilitate such comparisons, we first convert our data to heats of formation.

4.1. Heats of Formation (ΔH_f). To examine the energetics for various reaction mechanisms for hydrocarbon rearrangements it is useful to convert our calculated energetics to heats of formation (ΔH_f).

We can consider two extreme cases here:

(1) Low coverage: the H atoms released or required by the reaction go onto the surface. This may be more relevant in comparing to surface science experiments (low pressure).

(2) High coverage: the surface is saturated with H, which is in equilibrium with gas-phase H_2. This may be more relevant to practical catalysis experiments, which operate at significant partial pressures of H_2.

Although, differences of total energies calculated with QM correspond to changes in the internal energy (ΔU) of a system,

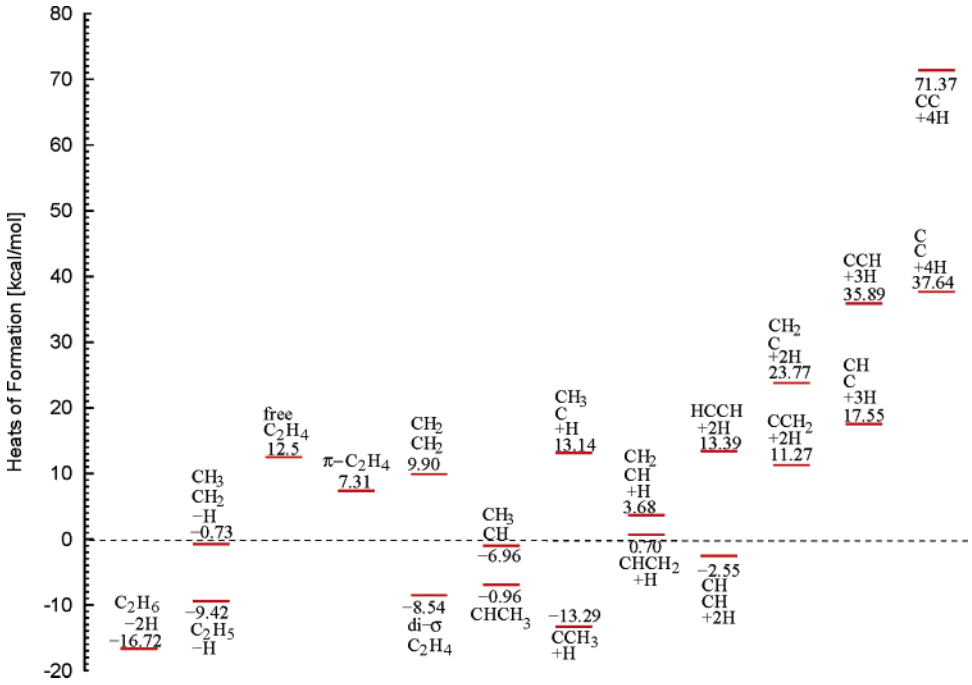

Figure 9. Heats of formation for various CH_x and C_2H_y species involved in decomposition and formation of C_2H_6 over Pt(111). This assumes low coverage conditions where any H atoms released in the reaction go to far surface sites.

the deviation from ΔH_f values is assumed to be rather small. Therefore, in the following we will assume ΔH_f values, which then allows us to be consistent with previous studies and experimental investigations (references, see below).

Normally the heat of formation ΔH_f is referenced to the standard state at 298K and atmospheric pressure. For the reactions of interest here the standard state would be bulk-fcc Pt, bulk graphite, and H_2 at STP. However, we find an alternative set to be more suitable for our calculations. It defines the needed reference energies (E_f) for Pt_{35}, H, and C as following:

(a) We consider the standard state of Pt to be the Pt_{35} cluster. Thus, $\Delta H_f(Pt_{35}) = 0$.

Since the QM total energy for the ground state of the Pt_{35} cluster is

$$E_{QM}(Pt_{35}) - 35 \times E_f(Pt) = 0$$

we can write for the Pt reference energy $E_f(Pt) = E_{QM}(Pt_{35})/35$. However, in this paper we only consider the Pt_{35} so that every equation will have $35 \times E_f(Pt) = E_{QM}(Pt_{35})$.

(b) We consider the standard state of H_2 to be the minimized energy of a free (gas-phase) H_2 molecule, $\Delta H_f(H_2) = 0$. Our QM total energy of H_2 is calculated to be

$$E_{QM}(H_2) - 2 \times E_f(H) = -1.17854h - 2 \times E_f(H) = \Delta H_f(H_2) = 0$$

leading to a reference energy for H of $E_f(H) = -0.58927h$.

(c) Finally, rather than bulk graphite we use gas-phase butane as the third reference point (for C). This has an experimental heat of formation of $\Delta H_f(C_4H_{10}) = -30.03$ kcal/mol.[28] To obtain the reference energy for carbon ($E_f(C)$), we write

$$E_{QM}(C_4H_{10}) - 4 \times E_f(C) - 10 \times E_f(H) = -158.46748h - 4 \times E_f(C) - 10 \times E_f(H) = -30.03 \text{ kcal/mol}$$

which leads to

$$E_f(C) = [E_{QM}(C_4H_{10}) - \Delta H_f(C_4H_{10}) - 10 \times E(H)]/4 = -38.13174h$$

Using butane to define the carbon reference energy differs from the choice of KG, who used $\Delta H_f(CH_4) = -17.9$ kcal/mol to define $E_f(C)$ for all CH_x species and used $\Delta H_f(CH_2CH_2) = +12.5$ kcal/mol[29] for all C_2H_y adsorbates. We use butane here because it is saturated with several C−C and C−H bonds, which we consider to provide a more reliable comparison for both CH_x and C_2H_y species.

The following illustrates an example how on the basis of the previous defined reference energies the heats of formation are calculated

$$\Delta H_f(CH_3/Pt_{35}) = E_{QM}(CH_3/Pt_{35}) - E_f(C) - 3 \times E_f(H) - E_f(Pt_{35})$$
$$= -4211.49553h - (-38.13174)h - 3 \times (-0.58927)h - (-4171.57547)h$$
$$= -0.02051h = -12.87 \text{ kcal/mol}$$

Similarly, the QM calculation for free CH_3 leads to $\Delta H_f(CH_3) = 37.03$ kcal/mol, leading to the bond energy to Pt of 49.89 kcal/mol.

The calculated heats of formation are given in Tables 1−3, where all calculations used this approach.

Similarly, we use the binding energy of chemisorbed H onto Pt_{35} of 62.49 kcal/mol to obtain the heat of formation for adsorbed hydrogen as $\Delta H_f(H/Pt_{35}) = -7.19$ kcal/mol.

We used these values to obtain the plots of Figures 9 and 10, in which the first diagram summarizes all heats of formation. There we assumed low coverage conditions in which any H atom dissociated from the fragment can bind to the surface at a distance far from the remaining hydrocarbon. This allows us to ignore interactions between the dissociation products. Hydrogen has similar binding energies at the various sites of the Pt(111) surface, leading to barriers of <2 kcal/mol, making them extremely mobile, so that this assumption is reasonable.

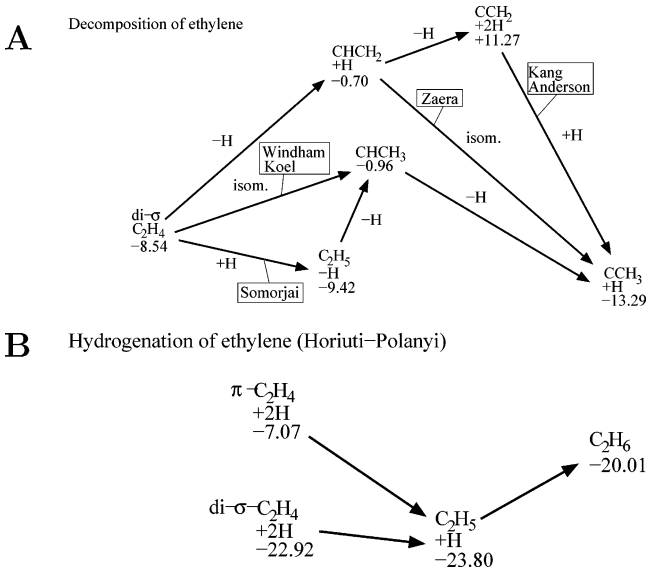

Figure 10. Upper diagram shows four different pathways for the decomposition of ethene to CCH_3, whereas the lower diagram shows the Horiuti and Polanyi mechanism for hydrogenation of ethene to ethane.

4.2. Comparison with Experiment for CH_x. Although there exist nearly no detailed experimental results on energetics and structures of the CH_x compounds, we can use the heats of formation to compare our results with different reactions, that have been examined experimentally.

Molecular beam surface scattering[30] and low-energy electron irradiation[31] experiments have been interpreted in terms of dissociative adsorption of methane to form adsorbed methyl and hydrogen, which can be enhanced by increasing the translational energy of methane or the surface temperature. Our calculations indicate that the reaction

$$(CH_4)^g \rightarrow H/Pt + CH_3/Pt$$

is exothermic by 2.16 kcal/mol, which is consistent with dissociative chemisorption. In addition, the low value agrees with the enhanced dissociative adsorption of methane for increased surface temperatures.[31] Quantum-dynamical modeling of CH_4 based on molecular beam experiments give an activation energy for methane adsorption of 17.53 kcal/mol,[32,33] whereas temperature-programmed desorption measurements (TPD) suggest a slightly lower activation of 17.06 kcal/mol for the back reaction.[34]

The adsorption site of methyl has been measured with high-resolution electron energy loss spectroscopy (HREELS) and reflection-adsorption infrared spectroscopy (RAIRS). From an analysis of the vibrational frequencies these experiments conclude that CH_3 has a local C_{3v} symmetry, suggesting either an on-top (μ_1) or a 3-fold (μ_3) adsorption site.[35−38] Our calculations show clearly that it is μ_1 (on-top).

The chemistry of methyl has been studied by TPD and RAIRS.[39] These studies found that the surface chemistry of methyl is dominated by hydrogenation (to form methane) and dehydrogenation (to form surface carbon finally), with both reactions competing. The energetics in Table 2 indicate that

$$CH_3/Pt + H/Pt \rightarrow (CH_4)^g$$

is endothermic by 2.16 kcal/mol, whereas

$$CH_3/Pt \rightarrow CH_2/Pt + H/Pt$$

is endothermic by 10.63 kcal/mol. These results are consistent with the competition between the two pathways seen experimentally. Based on these experiments it was proposed that since CH_2/Pt is more reactive than CH_3/Pt the final hydrogenation step to form methane is a multiple exchange reaction.[40] Since

$$CH_2/Pt + H/Pt \rightarrow (CH_3)/Pt$$

is exothermic by 10.63 kcal/mol, whereas

$$CH_2/Pt \rightarrow CH/Pt + H/Pt$$

is exothermic by 6.32 kcal/mol, it is plausible that adsorbed CH_2 undergoes reversible conversion to CH before the final hydrogenation to methane. This is consistent with the interpretation of the experiments.

Assuming bond additivity, the binding energies of CH, CH_2, and CH_3 lead to an average amount of 48.8 kcal/mol per Pt−C bond. This can be compared to microcalorimetric studies that suggest an intrinsic Pt−C bond energy of 54−64 kcal/mol.[41]

4.3. Comparison with Experiment for C_2H_y. *4.3.1. C_2H_4.* Because of its importance in heterogeneous catalysis, the most studied C_2H_y species is ethene. Various experimental approaches have been used to study the hydrogenation of ethene to form ethane and to study the decomposition of ethene. Among the intermediates formed in these reactions only three species have been characterized experimentally: (1) π-ethene (π-C_2H_4), (2) di-σ-ethene (di-σ-C_2H_4), and (3) ethylidyne (CCH_3) the latter of which was found to be the most stable.

Ultraviolet photoemission spectroscopy (UPS)[42] shows that ethene adsorbs as π-bonded species at low temperatures, but that heating above 52 K it transforms to di-σ-ethene. Since we find a 15.85 kcal/mol higher binding energy for the di-σ structure than for π-ethene, this is consistent with our results (but we find no conversion barrier). In case of π-ethene, RAIRS[43] experiments found a bond energy of 9.6 ± 2.4 kcal/mol, with the C═C double bond parallel to the surface. Our calculations of on-top adsorbed C_2H_2 (π-ethene) lead to a binding energy of 10.59 kcal/mol, with the C═C bond parallel to the surface.

HREELS,[44] UPS,[45] and near-edge absorption fine structure experiments (NEXAFS)[46] conclude that di-σ-ethene binds at a bridge site between two Pt atoms, and the C−C bond is 1.49 ± 0.04 Å (NEXAFS) and parallel to the surface (our result: 1.494 Å).

A variety of experimental values are available on the energetics. Early TPD experiments[47] found a desorption energy of 17 kcal/mol. Collision-induced desorption (CID) determined an upper limit of 48.4 ± 2.3 kcal/mol. This can be compared to our calculated bond energy for the di-σ state of 26.44 kcal/mol.

Experiments at temperatures above 280 K indicate that during the adsorption process ethene dissociates and rearranges to form ethylidyne (CCH_3).[48] King et al. performed microcalorimetry studies on single Pt crystals at 300 K[41] and measured a range of binding energies from (41.6 ± 1.0) kcal/mol below 0.1 monolayer (ML) to (29.6 ± 0.7) kcal/mol for higher coverage (<0.2 ML). King concluded that at low coverage ethylidyne and atomic hydrogen are formed, whereas the second value corresponds to adsorbed ethylidyne and gas-phase H_2. Dumesic et al. reported a value of 34.71-37.58 kcal/mol for the first

reaction.[49,50] This is certainly compatible with our calculations:

$$(C_2H_4)^g \xrightarrow{-31.19} H/Pt + CCH_3/Pt$$

$$(C_2H_4)^g \xrightarrow{-24.00} CCH_3/Pt + {}^1/_2H_2$$

At lower temperatures of 173 K more recent microcalorimetry experiments on Pt powder[49] found a value of 28.7 kcal/mol for the molecular adsorption of ethene. Our calculated binding energy of 26.44 kcal/mol for the di-σ state is compatible with these more recent experiments. The earlier calculations on Pt_8 by KG led to 36.05 kcal/mol, which is about 10 kcal/mol larger than our Pt_{35} results. This is consistent with CH_3/Pt being about 5 kcal/mol stronger for Pt_8 than for Pt_{35}.

4.3.2. CCH_3. As indicated in section 4.3.1 ethene shows dissociative adsorption at temperatures above 280 K, leading to ethylidyne (CCH_3) on the surface and hydrogen either on the surface or in gas-phase. Although our calculated energetics are in good agreement with experiment for both reactions, there exist no direct energetics for the chemisorbed ethylidyne.

Low-energy electron diffraction (LEED) studies[51,52] show that ethylidyne binds to the μ_3 fcc site with a C−C bond length of 1.50 ± 0.05 Å and a Pt−C distance of 2.00 ± 0.05 Å. Our studies give 1.489 Å (C−C) and 1.997 Å (Pt−C_a), in excellent agreement with experiment.

Above 450K Cs^+ reactive ion scattering showed that ethylidyne decomposes gradually to CH_2, CH, and finally C_n molecules, instead of desorbing as an intact molecule. Since C_a forms a strong bond to the Pt surface, it is reasonable that the ion collision (Cs^+) causes the C−CH_3 bond to break. Our calculations show the following energy changes:

$$CCH_3/Pt \xrightarrow{+19.24} C/Pt + CH_3/Pt \xrightarrow{+10.63} C/Pt + CH_2/Pt +$$
$$H/Pt \xrightarrow{-3.68} C/Pt + CH/Pt + 2H/Pt \xrightarrow{+20.09} 2C/Pt +$$
$$3H/Pt \xrightarrow{+33.73} CC/Pt + 3H/Pt$$

Since ethylidyne is the most stable C_2H_y species nearly all reaction steps are endothermic, which is consistent with the requirement of high temperatures.

4.3.3. HCCH and CCH_2. LEED studies on acetylene found a molecular adsorption at μ_3 sites.[53] The experimental C−C bond length varies between 1.35 and 1.39 Å (UPS),[45] and the C−C−H angle is 120−132°. We calculate a bond length of 1.389 Å, and an angle of 126.3°, in good agreement with experiment.

Adsorption energy measurements using microcalorimetry on Pt powder[49] at 173 K gave 50 kcal/mol, which can be compared with our value of 43.91 kcal/mol

$$(HCCH)^g \xrightarrow{-43.91} HCCH/Pt$$

At >280 K NMR[54] studies of acetylene adsorption show the existence of CCH_2 and HCCH on the surface with a ratio of about 3:1, indicating that CCH_2 is more stable on the Pt(111) surface. Our calculations lead to

$$HCCH/Pt \xrightarrow{2.11} CCH_2/Pt$$

for this conversion. Thus, even though gas-phase CCH_2 is 41.89 kcal/mol less stable than HCCH, they have nearly equal energies on the surface. That is, CCH_2 has a 44.01 kcal/mol higher binding energy than HCCH.

The same NMR experiments measured the C−C bond length of adsorbed CCH_2 to be 1.44 ± 0.05 Å,[54] in reasonable agreement with our calculations, which lead to a C−C distance of 1.392 Å and 87.92 kcal/mol binding energy.

4.4. Decomposition of Ethene. Four different pathways have been proposed for converting ethene to ethylidyne (Figure 10A). Starting from ethene, Somorjai[55] suggested a mechanism involving ethyl and ethylidene

$$\text{di-}\sigma\text{-}H_2C{=}CH_2/Pt + H/Pt \xrightarrow{-0.88} H_2CCH_3/Pt \xrightarrow{+8.46} CHCH_3/Pt +$$
$$H/Pt \xrightarrow{-12.33} CCH_3/Pt + 2H/Pt$$

Our calculated energetics (listed above) lead to only one endothermic step of just 8.46 kcal/mol for the Somorjai mechanism.

Kang and Anderson[56] suggested a pathway involving vinyl and vinylidene

$$\text{di-}\sigma\text{-}H_2C{=}CH_2/Pt \xrightarrow{+7.84} CHCH_2/Pt + H/Pt \xrightarrow{+11.77} CCH_2/Pt + 2H/Pt \xrightarrow{-24.56} CCH_3/Pt + H/Pt$$

Here our calculated energetics lead to two endothermic steps, totaling 19.61 kcal/mol and one final exothermic step.

Windham and Koel[47] proposed a pathway involving isomerization to ethylidene as the first step

$$\text{di-}\sigma\text{-}H_2C{=}CH_2/Pt \xrightarrow{+7.58} CHCH_3/Pt \xrightarrow{-12.33} CCH_3/Pt + H/Pt$$

This involves an endothermicity in the first step of 7.58 kcal/mol.

In contrast, the Zaera-scenario[57] has dehydrogenation to form vinyl and then the isomerization

$$\text{di-}\sigma\text{-}H_2C{=}CH_2/Pt \xrightarrow{+7.84} CHCH_2/Pt + H/Pt \xrightarrow{-12.59} CCH_3/Pt + H/Pt.$$

This also involves a first endothermic step of 7.84 kcal/mol.

Of course, to settle such mechanistic issues will require the barriers for the various reactions. However, comparing the different pathways and their limiting reaction step, the Kang-Anderson would likely not be competitive, while the reaction proposed by Windham and Koel is the most favorable. Indeed the three-step processes are unlikely because at low temperatures (170K) vinylidene readily transforms to ethene and ethyl undergoes β-H elimination.[6] Thus, the Windham and Koel pathway seems to be most plausible.

Recent Cs^+ reactive ion scattering (RIS) experiments give evidence that ethylidene is an intermediate in this reaction and that neither ethyl nor vinyl are formed.[58,59] This is consistent with our calculations, but inconsistent with the Kang-Anderson pathway.

4.5. Hydrogenation of Ethene. The mechanism of the catalytic reaction to form ethane out of ethene via direct hydrogenation (Figure 10B)

$$\text{di-}\sigma\text{-}H_2C{=}CH_2/Pt + 2H/Pt \xrightarrow{-0.88} C_2H_5/Pt + H/Pt \xrightarrow{+3.79} (C_2H_6)^g$$

was first proposed by Horiuti and Polanyi.[60] They suggested a pathway of two hydrogenation steps to form first an ethyl

radical, which desorbs from the surface as it is hydrogenated to ethane. Starting from di-σ-ethene, we find that the total reaction is slightly endothermic by +2.91 kcal/mol.

Indeed at higher coverage, the sites that stabilize di-σ-ethene may be saturated so that π-ethene is present. This would lead to a first step that is exothermic by 16.73 kcal/mol.

It is possible that ethylidyne could be formed as an intermediate

$$\text{di-}\sigma\text{-}H_2C{=}CH_2/Pt + 2H/Pt \xrightarrow{-4.75} CCH_3/Pt + 3H/Pt \xrightarrow{+12.33} CHCH_3/Pt + 2H/Pt \xrightarrow{-8.46} CH_2CH_3/Pt + 1H/Pt \xrightarrow{+3.79} (C_2H_6)^g$$

However, various ^{14}C labeling experiments,[61] deuterium labeling experiments,[57] and UHV techniques[62] find no evidence for stable ethylidyne as an intermediate. Our calculations reaffirm the results from KG that ethylidyne is the most stable of the C_2H_y species, making it an unfavorable intermediate.

5. Summary

From QM calculations using the $Pt_{14.13.8}$ cluster (previously established as a good model for reactions on the Pt(111) surface), we examined the adsorption of various CH_x and C_2H_y hydrocarbons. In each case, we find that the structures on the surface are comparable to gas-phase analogues in which some CH bonds are replaced with C−Pt σ bonds. The result is that monoradicals bond to μ_1 on-top sites, di-radicals bond to μ_2 bridging sites and tri-radicals bind to μ_3 fcc sites. Our results for structures and energetics are in good agreement with available experimental results, and make many predictions that are testable experimentally.

In addition, we used the calculated binding energies to predict the heats of formation for the different adsorbates. We then used these numbers to analyze such reactions as the hydrogenation and decomposition of ethene and the conversion of ethene to ethane. We believe that this level of computation, which is rather simple and fast, can be used to map out many other more complex chemistry.

We also used a combination of structure, energy, charge, and spin to provide an interpretation for the bonding of each intermediate. In nearly all cases, this interpretation involves covalent bonding between the adsorbates and the individual Pt atoms of the surface, but for some intermediates internal π bonds form donor−acceptor bonds. We hope that building such a chemical bonding perspective for chemisorption to metal surfaces will lead to ideas on how to design improved catalysts and nanoscale devices.

Acknowledgment. T.J. gratefully acknowledges support by the German academic exchange service (DAAD). This work was also supported by General Motors. The computation facilities of the MSC have been supported by grants from DURIP-ARO, DURIP-ONR, NSF (MRI), and IBM-SUR. In addition, the MSC is supported by grants from DoE (FETL, ASC ASAP), ARO-MURI, ONR-MURI, NIH, ONR, Chevron-Texaco, Beckman Institute, Seiko-Epson, and Asahi Kasei.

Supporting Information Available: Figures showing atom numbering in various layers and charge and spin density distributions. This material is available free of charge via the Internet at http://pubs.acs.org.

References and Notes

(1) Gates, B. C. *Catalytic Chemistry*; Wiley: New York, 1992.
(2) Scatterfield, C. N. *Heterogeneous Catalysis in Industrial Practise*; McGraw-Hill: New York, 1991.
(3) Masel, R. I. *Principles of Adsorption and Reaction on Solid Surfaces*; Wiley: New York, 1996.
(4) Somorjai, G. A. *Chem. Rev.* **1996**, 96, 1223.
(5) Somorjai, G. A. *Introduction to Surface Chemistry and Catalysis*; Wiley: New York, 1994.
(6) Zaera, F. *Langmuir* **1996**, *12*, 88.
(7) Jacob, T.; Muller, R. P.; Goddard, W. A., III. *J. Phys. Chem. B* **2003**, *107* (35), 9465.
(8) Kua, J.; Goddard, W. A., III. *J. Phys. Chem. B* **1998**, *102*, 9492.
(9) Becke, A. D. *J. Chem. Phys.* **1993**, *98* (7), 5648.
(10) Lee, C.; Yang, W.; Parr, R. G. *Phys. Rev. B* **1988**, *37*, 785.
(11) Slater, J. C. *Quantum Theory of Molecules and Solids, Vol. 4: The Self-Consistent Field for Molecules and Solids*; McGraw-Hill: New York, 1974.
(12) Becke, A. D. *Phys. Rev. A* **1988**, *38*, 3098.
(13) Vosko, S. H.; Wilk, L.; Nusair, M. *Can. J. Phys.* **1980**, *58*, 1200.
(14) Xu, X.; Goddard, W. A., III. *Proc. Natl. Acad. Sci. U.S.A.* **2004**, *101* (9), 2673.
(15) *Jaguar 4.2*; Schrödinger Inc.: Portland, Oregon, 2000.
(16) Hay, P. J.; Wadt, W. R. *J. Phys. Chem.* **1985**, *82*, 299.
(17) Goddard III., W. A. *Phys. Rev.* **1968**, *174*, 659.
(18) Kahn, L. R.; Goddard, W. A., III. *J. Chem. Phys.* **1972**, *56*, 2685.
(19) Melius, C. F.; Olafson, B. D.; Goddard, W. A., III. *Chem. Phys. Lett.* **1974**, *28*, 457.
(20) Melius, C. F.; Goddard, W. A., III. *Phys. Rev. A* **1974**, *10*, 1528.
(21) Kittel, Ch. *Einführung in die Festkörperphysik*; R. Oldenbourg Verlag: München, 1991.
(22) McAdon, M. H.; Goddard, W. A., III. *Phys. Rev. Lett.* **1985**, *55*, 2563.
(23) Papoian, G.; Nørskov, J. K.; Hoffmann, R. *J. Am. Chem. Soc.* **2000**, *122*, 4129.
(24) Seetula, J. A.; Russell, J. J.; Gutman, D. *J. Am. Chem. Soc.* **1990**, *112*, 1347.
(25) Seakins, P. W.; Pilling, M. J.; Niiranen, J. T.; Gutman, D.; Krasnoperov, L. N. *J. Phys. Chem.* **1992**, *96*, 9847.
(26) Voter, A. F.; Goddard, W. A., III. *Chem. Phys.* **1985**, *98* (1), 7.
(27) Zaera, F. *Langmuir* **1991**, *7*, 1998.
(28) Pittam, D. A.; Pilcher, G. J. *Chem. Soc., Faraday Trans. 1* **1972**, *68*, 2224.
(29) Chase, M. W., Jr.; Davies, C. A.; Downey, J. R., Jr.; Frurip, D. J.; McDonald, R. A.; Syverud, A. N. *J. Phys. Chem. Rev. Data* **1985**, *14* (Suppl, 1), 1.
(30) Valden, M.; Xiang, N.; Pere, J.; Pessa, M. *Appl. Surf. Sci.* **1996**, *99*, 83.
(31) Alberas-Sloan, D. J.; White, J. M. *Surf. Sci.* **1996**, *365*, 212.
(32) Luntz, A. C.; Harris, J. *Surf. Sci.* **1991**, *258*, 397.
(33) Harris, J.; Simon, J.; Luntz, A. C.; Mullins, C. B.; Rettner, C. T. *Rhys. Rev. Lett.* **1991**, *67*, 652.
(34) Zaera, F. *Surf. Sci.* **1992**, *262*, 335.
(35) Oakes, D. J.; Newell, H. E.; Rutten, F. J. M.; McCoustra, M. R. S.; Chesters, M. A. *J. Vac. Sci. Technol.* A **1996**, *14*, 1439.
(36) Wenger, J. C.; McCoustra, M. R. S.; Chesters, M. A. *Surf. Sci.* **1996**, *360*, 93.
(37) Fan, J.; Trenary, M. *Langmuir* **1994**, *10*, 3649.
(38) Sheppard, N.; De La Cruz, C. *Adv. Catal.* **1998**, *42*, 181.
(39) Fairbrother, H. D.; Peng, X. D.; Trenary, M.; Stair, P. C. *J. Chem. Soc., Faraday Trans.* **1995**, *91*, 3691.
(40) Kemball, C. *Catal. Rev.* **1971**, *5*, 33.
(41) Yeo, Y. Y.; Stuck, A.; Wartnaby, C. E.; King, D. A. *Chem. Phys. Lett.* **1996**, *259*, 28.
(42) Cassuto, A.; Kiss, J.; White, J. M. *Surf. Sci.* **1991**, *255*, 289.
(43) Kubota, J.; Ichihara, S.; Kondo, J. N.; Domen, K.; Hirose, C. *Surf. Sci.* **1996**, *357/358*, 634.
(44) Steininger, H.; Ibach, H., Lehwald, S. *Surf. Sci.* **1982**, *17*, 685.
(45) Felter, T. E.; Weinberg, W. H. *Surf. Sci.* **1981**, *103*, 265.
(46) Stohr, J.; Sette, F., Johnson, A. L. *Phys. Rev. Lett.* **1984**, *53*, 1684.
(47) Windham, R. G.; Bartram, M. E.; Koel, B. E. *J. Phys. Chem.* **1988**, *92*, 2862.
(48) Sheppard, N.; de la Cruz, C. *Adv. Catal.* **1996**, *41*, 1.
(49) Spiewak, B. E.; Cortright, R. D.; Dumesic, J. A. *J. Catal.* **1998**, *176*, 405.
(50) Watwe, R. M.; Cortright, R. D.; Nørskov, J. K.; Dumesic, J. A. *J. Chem. Phys. B* **2000**, *104*, 2299.
(51) Starke, U.; Barbieri, A.; Materer N.; van Hove, M. A.; Somorjai, G. A. *Surf. Sci.* **1993**, *286*, 1.
(52) Kesmodel, L. L.; Dubois, J. H.; Somorjai, G. A. *J. Chem. Phys.* **1979**, *70* (5), 2180.
(53) Kesmodel, L. L.; Baetzold, R. C.; Somorjai, G. A. *Surf. Sci.* **1977**, *66*, 299.

(54) Wang, P.-K.; Slichter, C. P.; Sinfelt, J. H. *Phys. Rev. Lett.* **1984**, *53* (1), 82.
(55) Somorjai, G. A.; van Hove, M. A., Bent, B. E. *J. Phys. Chem.* **1988**, *92*, 973.
(56) Kang, D. B.; Anderson, A. B. *Surf. Sci.* **1985**, *155*, 639.
(57) Zaera, F. *J. Phys. Chem.* **1990**, *94*, 5090.
(58) Hwang, C. H.; Lee, C. W.; Kang, H.; Kim, C. M. *Surf. Sci*. **2001**, *490* (1−2), 144.
(59) Kang, H.; Lee, C. W.; Hwang, C. H.; Kim, C. M. *Appl. Surf. Sci.* **2003**, *203*−*204*, 842.
(60) Horiuti, J.; Polanyi, M. *Trans. Faraday Soc.* **1934**, *30*, 1164.
(61) Davis. S. M.; Zaera, F.; Gordon, B.; Somorjai, G. A. *J. Catal.* **1985**, *92*, 250.
(62) Cremer, P. S.; Su, X.; Shen, Y. R.; Somorjai, G. A. *J. Am. Chem. Soc.* **1996**, *118*, 2942.